Fachtagung „Experimentelle Strömungsmechanik“
05.-07.09.2017, Karlsruhe

Einfluss einer zweiten gasförmigen Phase auf die Lorentzkraft-Anemometrie bei schwach leitfähigen Fluiden

Influence of a second gaseous phase on Lorentz force velocimetry at low conducting fluids

Andreas Wiederhold and Christian Resagk

Institut für Thermodynamik und Fluidmechanik, Technische Universität Ilmenau
Am Helmholtzring 1, 98693 Ilmenau

Schlagworte: Lorentzkraft-Anemometrie, Zweiphasenströmung, Blasendetektion
Key words: Lorentz force velocimetry, two-phase flow, bubble detection

Abstract

Lorentz force velocimetry (LFV) is a contactless and non-invasive flow measurement technique which has been developed and demonstrated for numerous applications in our institute and in industry. When an electrical conducting fluid passes a magnetic field Lorentz forces are generated. These forces are proportional to the electrical conductivity, to the velocity of the fluid and to the square of the magnetic flux density. Therefore it is possible to apply this technique to liquid metals where the conductivities are comparable with them of metals and for electrolytes, which is more challenging because the forces are six orders smaller. After we have shown that LFV is insensitive to different velocity profiles and strongly asymmetric profiles, in the next step the influence of a second gaseous phase on the force signal will be investigated. This is of fundamental interest especially for chemical and food processing industries. For this purpose different air flow rates are injected into the test section. By using frits it is possible to generate a homogeneous distribution of the second phase in the electrolyte. Small velocities of the electrolyte ($u < 1.5$ m/s) enable the formation of stratified wavy flow and higher velocities ($u > 1.8$ m/s) the formation of bubbly two-phase flow. By this means is it possible to study a wide range of flow patterns in horizontal duct flow. In a second approach the influence of elongated bubbles to LFV is investigated. Here a superposition of Lorentz forces and magnetic forces, which occur because of the different magnetic susceptibilities between the electrolyte and air, could be identified. We show that these magnetic forces can be used to measure geometry parameters like length and height and the velocity of the bubble. Furthermore it is possible to apply this method to solid bodies where inclusions or defects in diamagnetic and paramagnetic material can be detected. This opens up new possibilities in the field of nondestructive material testing (NDT).

Introduction

Dispersed two-phase flow is important in a wide range of laboratory and industrial processes, e.g. in heat exchangers, nuclear reactors or oil pipelines. Furthermore over 50 % of the products produced by chemical industries are of dispersed nature [1]. After we have shown that LFV, a contactless flow measurement technique for electrical conducting fluids, is insensitive to different velocity profiles [2], now we want to study the influence of a second gaseous phase to LFV. This second phase can be large slugs or the gas is distributed homogeneously in the electrolyte. Many flow measurement techniques are susceptible to a second phase, because either they are invasive or the optical access will be disturbed. We

Karlsruhe, Germany, ISBN 978-3-9816764-3-3

show that it is possible to apply LFV to two-phase flow and furthermore to detect and to measure slugs with the help of magnetic forces [3, patent pending].

Theory

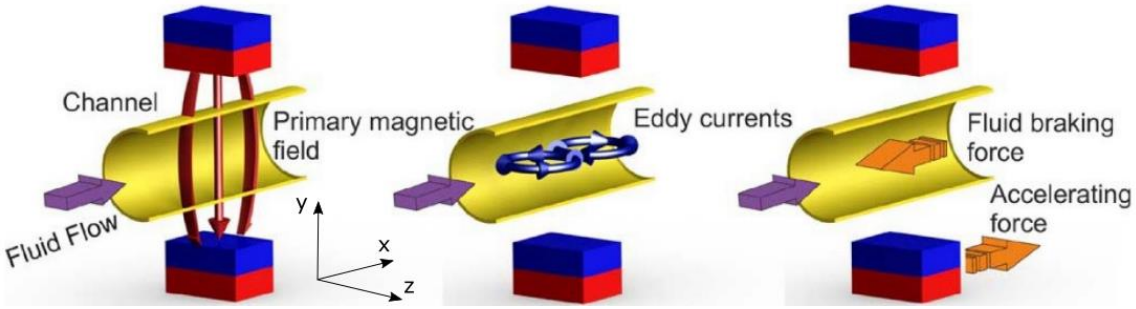

Figure 1. Principle of Lorentz force velocimetry: The fluid flow is exposed to a static magnetic field and hence, eddy currents are generated. The resulting force on the source of the primary magnetic field is an accelerating force in the direction of flow. This force is called Lorentz force.

The basic principle of LFV is as follows: An external magnetic field induces eddy currents in a passing fluid (see figure 1). Because of the movement there is an interaction of these eddy currents with the primary magnetic field, which cause a breaking force to the fluid. As a result of Newton's 3rd law there is a drag force – the Lorentz force – on the magnets in the direction of the flow. The Lorentz force is proportional to the square of the magnetic flux density B, the flow velocity v and to the electrical conductivity of the fluid σ [4].

$$F_L \sim \sigma v\, B^2 \sim \sigma \frac{dV}{A \cdot dt}\, B^2 \qquad (1)$$

Because the second phase has a different magnetic susceptibility there acts a further magnetic force on the surface of a bubble. This force is proportional to the surface area of the bubble front, while entering the magnetic field, to the square of the magnetic flux density and to the difference of the magnetic susceptibilities [5].

$$F_M = -\frac{1}{2} h_b \cdot b \frac{B^2}{\mu_0} (\chi_2 - \chi_1) \qquad (4)$$

The direction of the force is dependent on the magnetism of the fluids. E.g. when an air bubble enters the magnetic field the force acts on the front side of the bubble. Because air is paramagnetic, its magnetic susceptibility is higher than that of the diamagnetic water.

Experimental setup

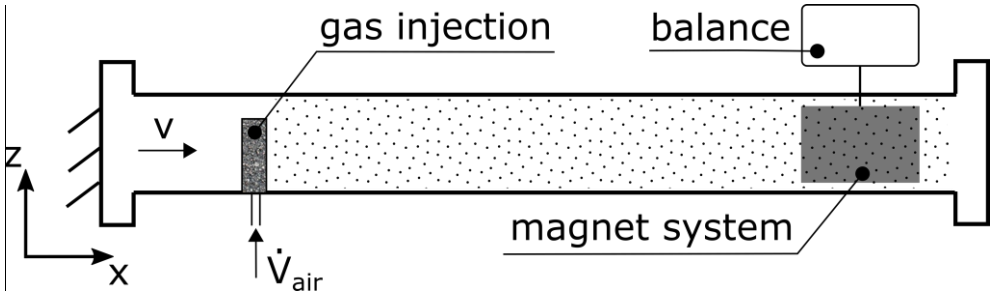

Figure 2: Sketch of the test section and the positions of the air supply and of the measurement system.

Karlsruhe, Germany, ISBN 978-3-9816764-3-3

In figure 2 the test section of the experimental setup is depicted, which is part of an electrolyte channel [6]. Three frits are inserted into the test section, which has a quadratic cross section, to inject air bubbles. Dependent on the flow velocity and the amount of the injected air three flow patterns can be studied: Slug flow, stratified flow and dispersed flow (figure 3a). The electrical conductivity of the fluid is σ = 20 S/m.

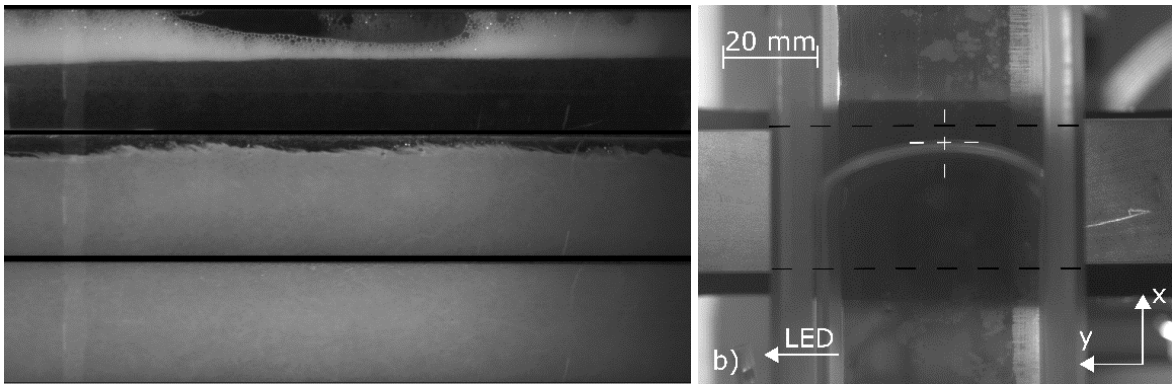

Figure 3: a) Different flow patterns: Slug flow (u = 0.4 m/s, V_{air} = 20 l/min), stratified flow (u = 1.4 m/s, V_{air} = 20 l/min), fully dispersed flow (u = 2.0 m/s, V_{air} = 20 l/min). b) Bottom view of elongated bubbles while passing the magnetic field which is confined by the dashed lines (neglecting stray field). When the bubble velocity increases the front of the bubble becomes blunted. The white cross indicates the foremost point of the bubble.

Furthermore we measure single air bubbles in tap water, which is practically nonconductive to study the magnetic forces acting on the bubbles surface. For this the test section is dismounted from the channel and closed at both ends, to enable an inclination. The moving bubbles are measured with a camera. The force measurement system consists of an electromagnetic force compensation balance (EMFC) [7] and magnet systems, which can be cubic magnets or Halbach arrays [8].

Measurement results and discussion

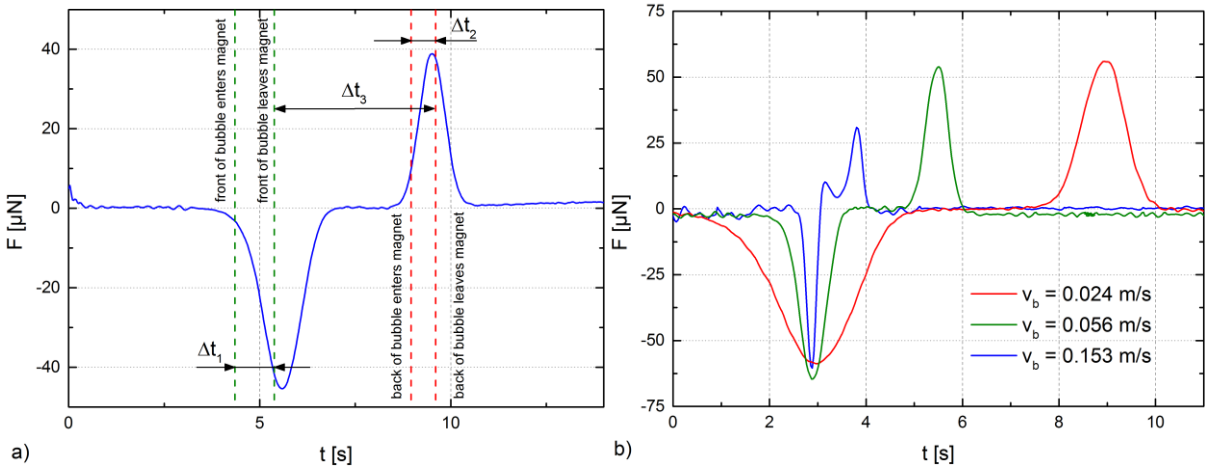

Figure 4: Typical force signal while a bubble passes the magnet (a). The green and red dashed lines indicate when the bubble front or back enters or leaves the region of the magnet system. Force signals for the measurement of elongated bubbles with a length of about 165 mm at different velocities with the classic magnet system (b).

Magnetic forces on elongated bubbles

First we present results of the single bubble measurements in tap water. In figure 4a the typical force signal is depicted while an elongated bubble is passing the magnetic field. Once the bubble front enters the magnetic field a negatice force peak appears and a positive force peaks appears when the back of the bubble leaves the magnetic field. These peaks can be used to measure the velocity and the length of the bubble by using the time differences indicated in figure 4 and the dimension of the magnetic field in x-direction. Furthermore it is possible to calculate the height of the bubble with the magnitude of these peaks. Figure 4b shows the force signals for an elongated bubbles at three different velocities.

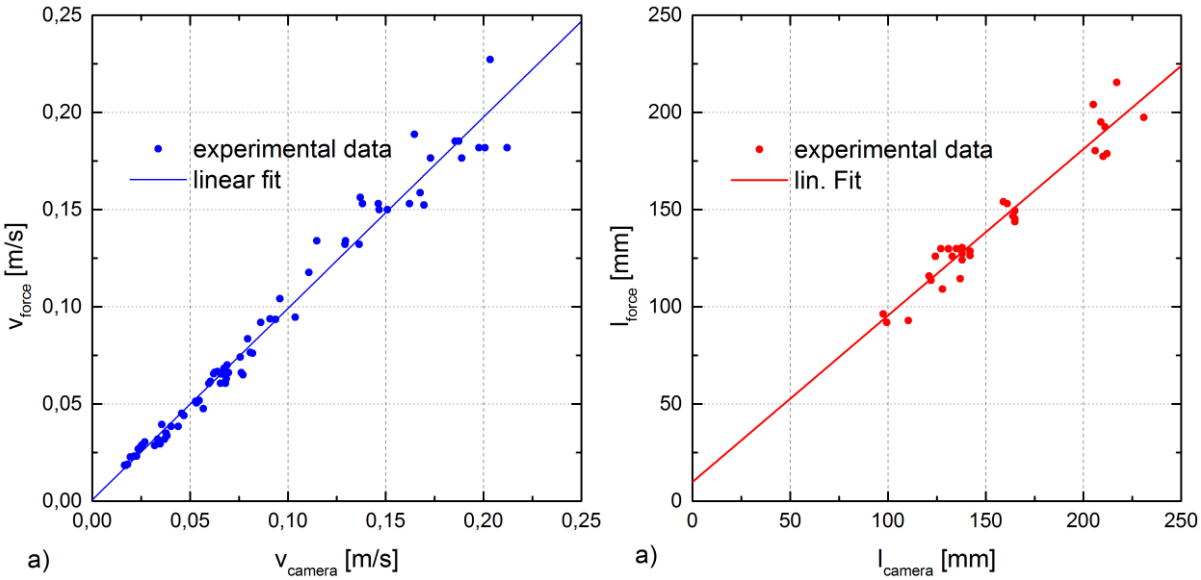

Figure 5: Comparison of the measured bubble velocities and bubble lengths between force measurements with the classic magnet system and camera measurements.

We have compared the velocities and lengths, obtained from the force measurement method with them of camera measurements (figure 5a/b). Both comparisons show a good one-to-one correspondence, high linearity and nearly no offset. When the velocity of the bubble increases, the experimental data show a stronger deviation, which could be explained by the temporal resolution of the camera measurements. The bubble length is calculated with the product of the time span between the two peaks Δt_3 and the already obtained bubble velocity v_B. The offset of the length measurement is larger, because of the error propagation of the velocity measurement.

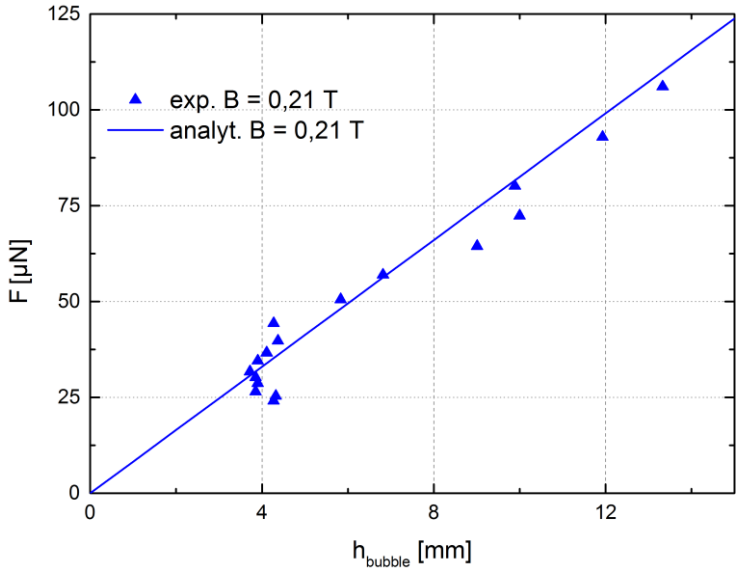

Figure 6: Comparison of the measured bubble velocities and bubble lengths between force measurements with the classic magnet system and camera measurements.

Furthermore it is possible to calculate the height of the bubble, provided that the bubble spans the whole width of the test section. We have calculated an averaged magnetic flux density of B = 0.21 T for the top region of the used magnets [8]. According to Eq. 2, there is a linear dependence of the force from the bubble height, which can be confirmed with the experimental data.
Not shown here are further measurements with oil drops in water and solid bodies, where defects are inserted. With the magnetic force method it is possible to detect defects in aluminum, plastic and glass specimen, which have dimensions in the order of 10^{-2} mm. This opens up new possibilities in the field of nondestructive material testing.

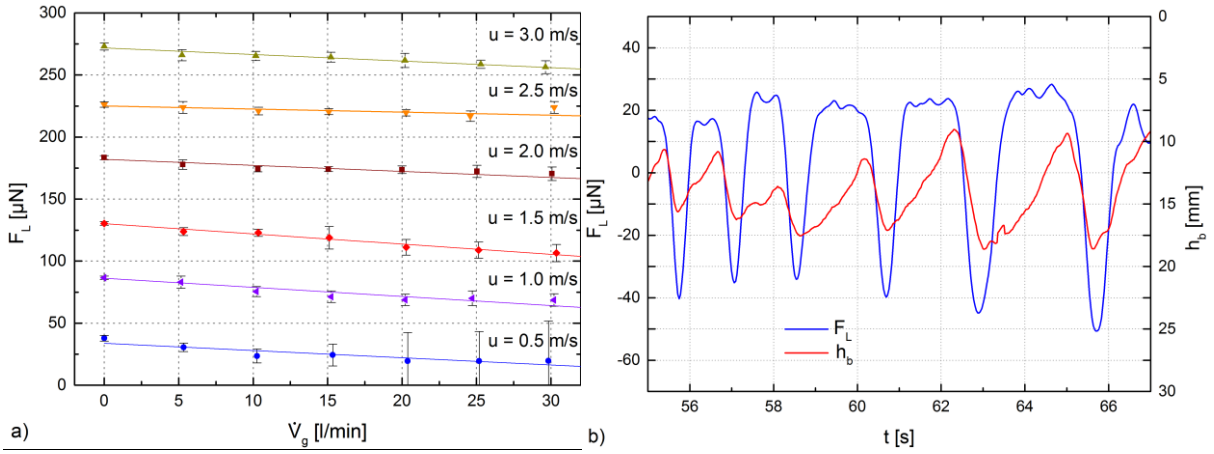

Figure 7: Lorentz forces at different air flow rates and flow velocities (a). Superposition of LFV measurement with magnetic forces at slug flow (b).

Lorentz force measurements

Figure 7a shows the measured Lorentz forces for different flow velocities and air flow rates. It is possible to cover a volumetric void fraction $\varepsilon = \dot{V}_l/(\dot{V}_l + \dot{V}_g)$ of 0 - 30 %, where $\dot{V}_g$ is the flow rate of air and $\dot{V}_l$ the flow rate of the electrolyte. At higher velocities (u > 1.5 m/s) the gaseous phase is fully dispersed, at lower velocities (u < 1.0 m/s) slug flow is present and stratified flow lies in between. The slug flow becomes noticeable through enlarged error bars. At all flow velocities a slight decrease in the force signal can be seen with increasing air flow $\dot{V}_g$, which can be explained by the electrical nonconductive air.

In figure 7b illustrates a superposition of Lorentz forces and magnetic forces in the slug flow regime. There is a large drop of the Lorentz force when a single slug is passing the magnetic field. To verify this we have measured the height of the interface between the electrolyte and the air (red curve), which correlates with the force signal.

Conclusions and outlook

The influence of a second gaseous phase to LFV has been investigated. Different flow conditions have been measured, which show specific behavior. Single bubbles and large slugs lead to a magnetic force, which acts on the bubble surface. With the help of this force it is possible to detect and to measure the velocity and geometry parameters of the bubble. If the gaseous phase is distributed homogeneously in the electrolyte the magnetic force is compensated and only a slight decrease of the Lorentz force can be measured. This decrease is in accord with the expected forces, considering a linear influence of the void fraction ε on the Lorentz force measurements. This is advantageous for industrial processes to measure the volume fraction of the gaseous phase in two-phase flow.

Acknowledgements

The authors are grateful to the German Science Foundation (Deutsche Forschungsgemeinschaft) for financial support of the presented work in the framework of the 'Lorentz force velocimetry and Lorentz force eddy current testing' Research Training Group (GRK 1567) at Technische Universität Ilmenau. We thank Markus Weidner for assisting in developing the magnetic force method and fruitful discussions.

References

1. H. Schubert. *Handbuch der Mechanischen Verfahrenstechnik*. Wiley-VCH, 2002, pp. 8-9.
2. A. Wiederhold et al. ”Influence of the flow profile to Lorentz force velocimetry for weakly conducting fluids - an experimental validation.” *Measurement Science and Technology*, 2016, vol. 27, no. 12.
3. A. Wiederhold and M. Weidner, “Verfahren und Vorrichtung zur Ermittlung der Anzahl, der Bewegungsgeschwindigkeit und der Größe von Defekten in einem strömenden Fluid“, Germany Patent 10 2017 002 035.3 (pending), February 27, 2017.
4. A. Thess et al. “Theory of the Lorentz force flowmeter.” *New Journal of Physics,* 2007, vol. no. 8, 299.
5. A. Zangwill. *Modern Electrodynamics*. Cambridge University Press, 2013, p. 439.
6. A. Wegfraß. “Experimentelle Untersuchungen zur Anwendbarkeit der Lorentzkraft-Anemometrie auf schwach leitfähige.“ PhD Thesis, Technische Universität Ilmenau, Germany, 2013.
7. S. Vasilyan, M. Rivero, J. Schleichert, B. Halbedel and T. Fröhlich. “High-precision horizontally directed force measurements for high dead loads based on differential electromagnetic force compensation system.” *Measurement Science and Technology*, 2016, vol. 27, no. 4, 045107 (13pp).
8. M. Werner. “Design, Optimierung, Realisierung und Test von passiven Magnetsystemen für die Lorentzkraftanemometrie an Elektrolyten.“ PhD Thesis, Technische Universität Ilmenau, Germany, 2013.

Karlsruhe, Germany, ISBN 978-3-9816764-3-3